Haploinsufficiency of the NF-κB1 Subunit p50 in Common Variable Immunodeficiency

Manfred Fliegauf,[1] Vanessa L. Bryant,[2,3] Natalie Frede,[1] Charlotte Slade,[2,3,4] See-Tarn Woon,[5] Klaus Lehnert,[6] Sandra Winzer,[1] Alla Bulashevska,[1] Thomas Scerri,[2,3] Euphemia Leung,[7] Anthony Jordan,[8] Baerbel Keller,[1] Esther de Vries,[9] Hongzhi Cao,[10] Fang Yang,[10] Alejandro A. Schäffer,[11] Klaus Warnatz,[1] Peter Browett,[7] Jo Douglass,[2,4,12] Rohan V. Ameratunga,[5] Jos W.M. van der Meer,[13] and Bodo Grimbacher[1,14,*]

Common variable immunodeficiency (CVID), characterized by recurrent infections, is the most prevalent symptomatic antibody deficiency. In ~90% of CVID-affected individuals, no genetic cause of the disease has been identified. In a Dutch-Australian CVID-affected family, we identified a *NFKB1* heterozygous splice-donor-site mutation (c.730+4A>G), causing in-frame skipping of exon 8. *NFKB1* encodes the transcription-factor precursor p105, which is processed to p50 (canonical NF-κB pathway). The altered protein bearing an internal deletion (p.Asp191_Lys244delinsGlu; p105ΔEx8) is degraded, but is not processed to p50ΔEx8. Altered NF-κB1 proteins were also undetectable in a German CVID-affected family with a heterozygous in-frame exon 9 skipping mutation (c.835+2T>G) and in a CVID-affected family from New Zealand with a heterozygous frameshift mutation (c.465dupA) in exon 7. Given that residual p105 and p50—translated from the non-mutated alleles—were normal, and altered p50 proteins were absent, we conclude that the CVID phenotype in these families is caused by NF-κB1 p50 haploinsufficiency.

Introduction

Common variable immunodeficiency (CVID1 [MIM: 607594], see this entry for additional MIM numbers for CVID2–CVID11) is a clinically and genetically heterogeneous disorder with an estimated incidence of 1:10,000–1:50,000.[1] CVID is the most frequent symptomatic primary immunodeficiency and is characterized by recurrent infections due to hypogammaglobulinemia and by deficiency of IgA and/or IgM. Recurrent pneumonia due to bacterial infection is the most common feature at initial presentation, and specific antibody responses are severely impaired. There is an increased prevalence of autoimmune disorders in CVID, and lymphoproliferative conditions are frequently observed.[2,3]

The milder disorder, selective IgA deficiency (sIgAD), has an incidence of 1:600–1:800, which is higher than that of CVID. Approximately 10% of CVID-affected family members will also have a relative with sIgAD,[4,5] which shares common susceptibility loci[6] with, and can progress to, CVID.[7–9] Similarly, within CVID-affected families, individual members might be diagnosed with hypogammaglobulinemia, a CVID-like disorder, or "possible" or "probable CVID" when they do not fulfill the diagnostic criteria for CVID.[2,10,11] Because diagnosis of CVID is established largely by exclusion— ruling out alternative causes for hypogammaglobulinemia— the CVID cohort is heterogeneous, comprising monogenic as well as polygenic disorders of variable origin.[2]

Although abnormal B and T cell functions are commonly observed in CVID, no genetic basis of these immune defects has yet been identified in the majority of these cases. Most CVID-affected individuals have reduced numbers of isotype-switched memory B cells, a severe reduction in post-germinal center B cells, and relative preservation of pre-germinal center B cells.[12] A potential role for regulatory T cells (Treg) in the pathogenesis of CVID has been suggested, given that affected individuals collectively have significantly lower Treg counts than unaffected control individuals do,[13,14] and a defect in Treg function has been demonstrated in some CVID-affected persons with mutations in *CTLA4*[15] (MIM: 123890). A genetic defect has been identified in only ~10% of CVID-affected individuals;[16,17] these defects include mutations in *ICOS* (inducible costimulator [MIM: 607594]), *TNFRSF13B* (which encodes TACI, a transmembrane activator and calcium-modulator and cyclophilin ligand interactor [MIM: 240500]), *CD19* (MIM: 613493), *BAFF-R* (B cell activating factor receptor; *TNFRSF13C* [MIM: 613494]), and several others. However, the molecular mechanisms leading to cellular defects and insufficient antibody production are poorly understood.

[1]Center for Chronic Immunodeficiency, University Medical Center Freiburg and University of Freiburg, Freiburg 79108, Germany; [2]Division of Immunology, Walter and Eliza Hall Institute of Medical Research, Parkville, VIC 3052, Australia; [3]Department of Medical Biology, The University of Melbourne, Parkville, VIC 3010, Australia; [4]Department of Clinical Immunology and Allergy, Royal Melbourne Hospital, Parkville, VIC 3050, Australia; [5]Department of Virology and Immunology, Auckland City Hospital, Auckland 1023, New Zealand; [6]School of Biological Sciences, University of Auckland, Auckland 1142, New Zealand; [7]Auckland Cancer Society Research Centre and Molecular Medicine and Pathology Department, University of Auckland, Auckland 1142, New Zealand; [8]Department of Clinical Immunology, Auckland City Hospital, Auckland 1023, New Zealand; [9]Department of Pediatrics, Jeroen Bosch Hospital, 's-Hertogenbosch 5200 ME, the Netherlands; [10]BGI–Shenzhen, Shenzhen, 518083, China; [11]NCBI, NIH, Department of Health and Human Services, Bethesda, MD 20894, USA; [12]Department of Medicine, The University of Melbourne, Parkville, VIC 3010, Australia; [13]Department of Internal Medicine, Radboud University Medical Centre, Nijmegen 6525 HP, the Netherlands; [14]Institute of Immunity and Transplantation, University College London, London WC1E 6BT, UK

*Correspondence: bodo.grimbacher@uniklinik-freiburg.de

http://dx.doi.org/10.1016/j.ajhg.2015.07.008.

Signaling via NF-κB (nuclear factor of kappa light polypeptide gene enhancer in B cells) is involved in a multitude of biological processes, including immune responses during inflammation, cell development and survival, and stress responses.[18–20] In B cell differentiation and function, both the canonical and the non-canonical NF-κB signaling pathways play pivotal roles.[21–23] The NF-κB transcription-factor family comprises five members, including NF-κB1 (the mature p50 and its precursor, p105), NF-κB2 (the mature p52 and its precursor, p100), RelA (p65), RelB, and c-Rel. These assemble into various homo- and heterodimeric combinations to regulate the expression of a large number (>500) of target genes, including those of cytokines, chemokines, growth factors, apoptosis regulators, cell surface receptors, and other transcription factors.

The five NF-κB proteins share in their sequences a Rel homology domain (RHD) in their N-terminal portions. The RHD mediates dimerization, interaction with each protein's specific inhibitors, and DNA binding. Following phosphorylation and poly-ubiquitination within the C-terminal portion of the protein, p105 and p100 undergo co- and/or posttranslational proteasomal processing into p50 and p52 subunits, respectively, and the processed subunits retain the RHD (Figure S1). In unstimulated cells, both the inactive NF-κB precursors and the NF-κB dimers that are associated with inhibitory proteins (IκBα, IκBβ, and IκBγ) are sequestered within the cytoplasm and therefore remain transcriptionally inactive.[18,21,24] Rapid activation of NF-κB occurs in response to numerous stimuli, typically with proteasomal degradation of IkBα (NF-kappa-B inhibitor alpha) in the canonical NF-κB pathway and partial proteolysis of p100 to p52 in the non-canonical NF-κB pathway.

NFKB1 (MIM: 164011) encodes p105 (969 amino acids), which is processed to the active subunit p50 (433 amino acids). In the canonical pathway, p50 assembles a heteromeric transcription factor, predominantly with RelA, that is complexed with IκBα. Upon stimulation of the canonical pathway by cytokines such as TNFα and IL-1, bacterial products (e.g., lipopolysaccharide), antigen receptors, or CD40L, the inhibitory κB kinase (IKK) of the NEMO-IKK complex becomes activated, which subsequently leads to phosphorylation of the inhibitory IκBα protein, poly-ubiquitination, and degradation by the 26S proteasome. The active p50-RelA dimer is then released, translocates to the nucleus, and binds to the promoters of its target genes.[24] For transcriptional activation, p50 is required to heterodimerize with RelA, which contains a transactivation domain. In contrast, homodimers of p50 lack a transactivation domain and act as transcriptional repressors. Transcriptional activation via the canonical pathway is characterized by instant and reversible expression of target genes encoding inflammatory cytokines, such as IL-6, and immune response genes.

Excessive or constitutive NF-κB activation has been implicated in various human malignancies, including solid tumors, acute and chronic leukemia, and B and T cell lymphomas.[25,26] Genetic lesions that directly cause impaired regulation of NF-κB-dependent signaling and are associated with one or more immunodeficiencies include those on genes *NFKBIA*[27,28] (*IKBA* [MIM: 164008]), *IKBKB*[29–31] (MIM: 603258), *IKBKG*[32,33] (*NEMO* [MIM: 300248]), *CARD9*[34] (MIM: 607212), *CARD11*[35] (MIM: 607210), *NOD2*[36,37] (*CARD15* [MIM: 605956]), *NLRP3*[38] (*CIAS1* [MIM: 606416]), and others.[19,20,39] A promoter polymorphism in *NFKB1* (−94 in/del ATTG [rs28362491]) has been associated with increased susceptibility to inflammatory bowel disease and/or ulcerative colitis (MIM: 266600).[40,41] B cell maturation, survival, differentiation, and T-cell-independent antibody class switching are associated with NF-κB-mediated signaling.[42,43] Furthermore, known disease-associated CVID genes, e.g., *TNFRSF13B* (encodes TACI [MIM: 604907]) and *TNFRSF13C* (encodes BAFF-R [MIM: 606269]), encode receptors that signal via the NF-κB pathways.[44,45]

In B cells, TACI signaling is a potent inducer of the canonical NF-κB1 pathway, whereas BAFF-R signaling mainly activates the non-canonical NF-κB2 pathway. Recent studies have identified *NFKB2* mutations (MIM: 164012) in CVID (MIM: 615577);[46–51] however, mutations in *NFKB1* have not yet been reported.

We have previously described a five-generation Dutch-Australian family with autosomal-dominant inheritance of CVID[52] and established an 18.7-Mbp linkage interval on chromosome 4q. However, in a candidate gene analysis (that included *NFKB1*), no mutations were identified by Sanger sequencing in coding exons within the linkage region. In the present study, we identified, by whole-exome sequencing (WES), a heterozygous splice-donor-site mutation in intron 8 of *NFKB1* that segregates with disease status in this CVID-affected family. The altered protein, p105ΔEx8, which results from in-frame skipping of exon 8, is rapidly degraded, and processing to p50ΔEx8 was undetectable. Subsequent targeted next-generation sequencing (NGS) identified a heterozygous splice-donor-site mutation in intron 9 of *NFKB1* in a German family affected by CVID. Analogously, in-frame skipping of exon 9 does not lead to the production of detectable amounts of an altered p50ΔEx9 protein. Furthermore, by WES, we identified a heterozygous single-base-pair duplication in exon 7 of *NFKB1* in a CVID-affected family from New Zealand. A severely truncated, non-functional protein, which might have been predicted and delineated from the mutant sequence, was undetectable. Our observations demonstrate that haploinsufficiency of the NF-κB1 subunit p50 is associated with a CVID phenotype.

Material and Methods

This study was conducted under protocols for human subjects, and samples were collected with the written consent of all study participants and/or their parental guardians after formal ethical approval by the local ethics committees at the University of Freiburg, the Radboud University, Melbourne Health, the University of Auckland, and collaborating institutions.

Cell Culture and Transfection

Peripheral blood mononuclear cells (PBMCs) were isolated and immortalized and Epstein-Barr virus (EBV)-transformed B-lymphocyte cultures were prepared according to standard procedures. Cells were cultured in RPMI 1640 Medium and supplemented with 10% fetal bovine serum and 1% penicillin-streptomycin (Invitrogen). For stimulation experiments, phorbol 12-myristate 13-acetate (PMA; 125 ng/μl in dimethyl sulfoxide; Sigma) and ionomycin (500 ng/μl in ethanol; Sigma) were added directly to the cell cultures (final concentrations: 50 ng/ml PMA and 1 μg/ml ionomycin) or CD40L (100 ng/ml MegaCD40L; Enzo Life Sciences, Sapphire Bioscience) and cells were harvested after incubation at 37°C as indicated. HEK293T and mouse fibroblasts (NIH 3T3 cells) were grown in Dulbecco's modified Eagle's medium supplemented with 10% fetal calf serum and 1% penicillin-streptomycin. Cells were plated onto collagen-coated coverslips and transfected with X-tremeGENE 9HP reagent (Roche), according to the suppliers' recommendations.

Sequence Analysis

Genomic DNA was isolated from blood samples with QIAamp Kits (QIAGEN). For mutational analysis in family FamNL1, WES was performed at BGI– Shenzhen and the Australian Genome Research Facility. Variants were annotated with an in-house annotation software system. Within the previously specified linkage region on chromosome 4q, a single unknown single-nucleotide variant (SNV) was identified, including a splice-donor-site mutation of intron 8 in *NFKB1*. A 582-bp genomic fragment of *NFKB1* comprising exon 8 and both intron and exon boundaries was amplified by PCR with the primers 5′-GAGGGA GGCGATC TGATACA-3′ (forward) and 5′-CTGGACATCAACCTTTCAAGC-3′ (reverse). In family FamNZ, a 370-bp amplicon encompassing the mutation in exon 7 was amplified by PCR with primers 5′-AAT TTA CAAGTGAAGCCAGAT-3′ and 5′-AAAAGGTGACAGCAGT GTG-3′. In family Fam089, a 281-bp genomic fragment spanning exon 9 was amplified by PCR with the primers 5′-AGGGGA GGGTCCTACCTAAAG-3′ (forward) and 5′-CTTGTCCACTGCTGA AATGTG-3′ (reverse). PCR primers were used for Sanger sequencing according to standard techniques.

cDNA Sequencing

RNA was isolated from EBV-transformed B cells with an RNeasy Mini Kit (QIAGEN) and reverse transcribed with Omniscript (QIAGEN) or Superscript III (Invitrogen). In FamNL1, a 649-bp cDNA fragment spanning exons 7–10 was amplified by PCR and sequenced with the primers 5′-GTGAGGATGGGATCTGC ACT-3′ (forward; exon 6) and 5′-CGAAGCTGGACAAACACAGA-3′ (reverse; exon 11). In Fam089, a 682-bp cDNA fragment spanning exons 8–11 was amplified and sequenced with the primers 5′-AAC ACTGGAAGCACG AATGAC-3′ (forward; exon 7) and 5′-ACT ACC ACC GCC GAA ACT ATC-3′ (reverse; exon 12).

Western Blotting

Cells were washed with PBS and lysed on ice in radioimmunoprecipitation assay buffer (50 mM Tris pH 8, 1% Igepal, 0.5% sodium-deoxycholate, 150 mM NaCl, 1 mM ethylenediaminetetraacetic acid [EDTA], 0.1% SDS, 1% protease inhibitor cocktail). Supernatants were separated on 4%–12% NuPAGE Bis-Tris gels (Invitrogen) and transferred onto polyvinylidene-difluoride membranes (Roche). p105 and p50 were detected with a rabbit antibody raised against the N terminus of NF-κB1 (#3035; Cell Signaling; NEB). Phosphorylated p105 was detected with a monoclonal rabbit antibody (#4806, Cell Signaling). Signals were detected with horseradish-peroxidase-coupled anti-rabbit secondary antibodies (NEB) via enhanced chemiluminescence (LumiGlo or SignalFire; NEB).

Preparation of Nuclear Extracts

Protein extracts enriched for nuclear proteins were prepared as previously described.[53] Cells were washed with PBS, resuspended in 400 μl of Buffer A (10 mM HEPES-KOH pH 7.9, 1.5 mM $MgCl_2$, 10 mM KCl, 0.5 mM dithiothreitol [DTT], 1% protease inhibitor cocktail; Sigma), and incubated on ice for 10 min. After brief vortexing and centrifugation, pellets were resuspended in 20–100 μl of Buffer C (20 mM HEPES-KOH pH 7.9, 25% glycerol, 420 mM NaCl, 1.5 mM $MgCl_2$, 0.2 mM EDTA, 0.5 mM DTT, 1% protease inhibitor cocktail) and incubated on ice for 20 min. Supernatants were collected and subjected to western blotting.

cDNA Expression Vectors and GFP-Fusion Constructs

The cDNAs encoding the full-length p105 (p105-FL) and the truncated p105ΔEx8 were both cloned by RT-PCR from EBV-transformed B lymphocytes derived from an affected individual harboring the heterozygous c.730+4A>G mutation. Restriction sites (XhoI and EcoRI) were introduced with the PCR primers. After sequence verification, the cDNAs were subcloned into pEGFP-C1 (Clontech, Takara) to generate GFP-fusion constructs. The cDNAs encoding p50 and p50ΔEx8 were generated by PCR from the p105-FL and truncated p105ΔEx8 versions, respectively. Non-fusion versions were obtained by subcloning into pEGFP-N1.

Fluorescence Staining and Confocal Imaging

Glass coverslips with transfected cells expressing GFP-p50, GFP-p50ΔEx8, GFP-p105-FL, or GFP-p105ΔEx8 fusion constructs were rinsed with PBS, and nuclei were stained with Hoechst 33342 (Sigma). Samples were mounted onto glass slides with fluorescence mounting medium (Dako) for microscopy. Confocal fluorescence images were taken on a Zeiss laser scanning microscope, LSM710, with an Axiovert 200M equipped with a 63× water immersion objective (Carl Zeiss). Images were evaluated and processed with the Zeiss ZEN blue-ZEN black software.

Identification of a Splice-Donor-Site Mutation in Intron 9 of *NFKB1* in a German Family by Targeted NGS

Genomic DNA was extracted from PBMCs of the proband (Fam089-II2). For target enrichment, commercial reagent kits were used according to the manufacturer's instructions (Agilent). DNA samples were treated with a restriction-enzyme master mix and the products were hybridized to the HaloPlex probe capture library including the indexing primer cassettes. The target DNA was captured by a biotin-streptavidin system with HaloPlex magnetic beads, and the circular fragments were closed in a ligation reaction. The captured target libraries were amplified by PCR, and the amplified target libraries were purified with AMPure XP beads (Beckman Coulter) and washed in ethanol. Enrichment was validated on a BioAnalyzer or TapeStation (Agilent). Subsequently, samples were pooled in equimolar amounts for multiplexed sequencing on an Illumina MiSeq system. Libraries were denatured and diluted to a final concentration of 8–12 pM. For sequencing, an Illumina Reagent Kit v.2 was used.

Identification of a *NFKB1* Frameshift Mutation in a CVID-Affected Family from New Zealand by Exome Sequencing

Genomic DNA was extracted from PBMCs of the male proband (FamNZ-II1), his mother (FamNZ-I2), and his affected sister (FamNZ-II2). Library preparation, exome enrichment (Nextera Rapid Capture Exome, Illumina), and exome sequencing (Illumina HiSeq 2000) was performed by New Zealand Genomics Limited. Approximately 59 million, 100-nucleotide paired-end reads were aligned to the 1000 Genomes Project reference genome (GRCh37.p13) with the Burrows-Wheeler aligner.[54] Duplicates were identified with Picard, followed by indel realignment and base-quality-score recalibration with the Genome Analysis Toolkit (GATK).[55] Final coverage of targeted intervals was 49-fold (49.2-, 49.2-, and 49.7-fold for the male proband, his mother, and his sister,respectively). Exome alignments from 44 unrelated individuals were added to support variant identification with GATK's HaplotypeCaller in "joint calling" mode and to empower variant quality-score recalibration.[56] A total of 63,486 high-confidence variants and 21,041 shared genotypes were detected in the three individuals. 6,018 shared variants were predicted to cause gain or loss of translation of start or stop codons, a frameshift, a codon insertion or deletion, or a non-synonymous amino-acid substitution or were located in consensus splice motifs or 5′- or 3′-untranslated regions. We removed variants exceeding an alternate allele frequency of 0.02 in the European subsets of the HapMap, 1000 Genomes Project, NHLBI GO Exome Sequencing Project, or Exome Aggregation Consortium (December 2014 version) cohorts, as well as variants with genotypes observed more than once in 125 in-house exomes (individuals with non-immunological phenotypes) and variants located in olfactory receptor genes. 79 variants were retained and analyzed for their disease-causing potential on the basis of the known biological roles, disease associations, and tissue expression of their genes, together with the predicted functional consequences of the individual mutations.

Results

Autosomal-Dominant Inheritance of a Heterogeneous Form of CVID in a Large Five-Generation Family

The index family (FamNL1, of Dutch origin) with multiplex CVID-sIgAD-hypogammaglobuliemia over five generations has previously been described.[52,57] The disease status, an overt late-onset hypogammaglobulinemia, segregated with an autosomal-dominant inheritance pattern. In the present study, additional family members have been included (Figure 1A), particularly one branch of the family, which migrated to Australia. FamNL1 is therefore referred to as a Dutch-Australian family. Clinical records have been reevaluated and follow-up examinations have been conducted, when possible. All study participants signed research informed consent forms after approval of the study by local research ethics committees. For those individuals who participated in both studies, the subject IDs are identical. The revised pedigree includes eleven individuals with CVID and nine with hypogammaglobulinemia. An update on the clinical phenotype of the affected family members is summarized in Table 1 and described in detail in the Supplemental Data case reports. The clinical histories are remarkably variable, ranging from moderate to severe hypogammaglobulinemia and from recurrent sinus infections to severe CVID characteristics, such as progressing pulmonary disease.

To localize the genetic defect in this family, a genetic linkage study was conducted in 2005, establishing an 18.7-Mbp linkage interval on chromosome 4q24.[52] The linkage interval was robust to various assumptions about whether individuals with milder phenotypes should be considered as "affected." Although the coding exons of several genes in the candidate region, including *NFKB1* (which spans ~116 kbp and comprises 23 coding exons plus a non-coding first exon [MIM: 164011]), were analyzed by Sanger sequencing, a disease-causing mutation was not identified. In light of our findings in the present study, the previous results might be attributed to an underestimation of sequence variants adjacent to the coding exons, such as the non-coding intronic splice sites, which were not exhaustively studied at that time.

Identification of a Splice-Donor-Site Mutation in Intron 8 of *NFKB1* by WES

Because a previous candidate-gene approach failed to identify disease-associated coding-sequence variants, we performed WES on two affected individuals (FamNL1-34 and FamNL1-49). In an independent approach, mutational analysis by exome sequencing was conducted in three additional family members (FamNL1-57, FamNL1-62, and FamNL1-64). Within the minimal linkage region (flanked by the microsatellite markers D4S2361 and D4S1572), only one single SNV was identified, namely an intronic sequence variant in *NFKB1* (g.103500200A>G; GRCh37). The sequence variant was not listed in the dbSNP, the Human Gene Mutation Database, the 1000 Genomes catalog, or the Exome Aggregation Consortium browser.

NFKB1 comprises 24 exons (Figure S1) and encodes two variants of the precursor protein p105 with 969 amino acids (variant 1 [GenBank: NM_003998.3]) and 968 amino acids (variant 2 [GenBank: NM_001165412.1]). The precursor undergoes proteasomal processing to produce p50 (433 amino acids). The identified sequence variant, c.730+4A>G (GenBank: NM_003998.3), affects the splice donor site of intron 8, suggesting that defective mRNA and/or protein synthesis might occur.

Segregation of the Heterozygous *NFKB1* Intron 8 Splice-Site Mutation with CVID Disease Status in FamNL1

To confirm that the identified *NFKB1* sequence variant segregates with disease status in the Dutch-Australian CVID-affected family, we analyzed genomic DNA from 35 affected and non-affected family members by Sanger sequencing of exon 8, including both exon and intron boundaries (Figure 1B). We found that all ten analyzed CVID-affected individuals and three family members with hypogammaglobulinemia (FamNL1-38, FamNL1-42,

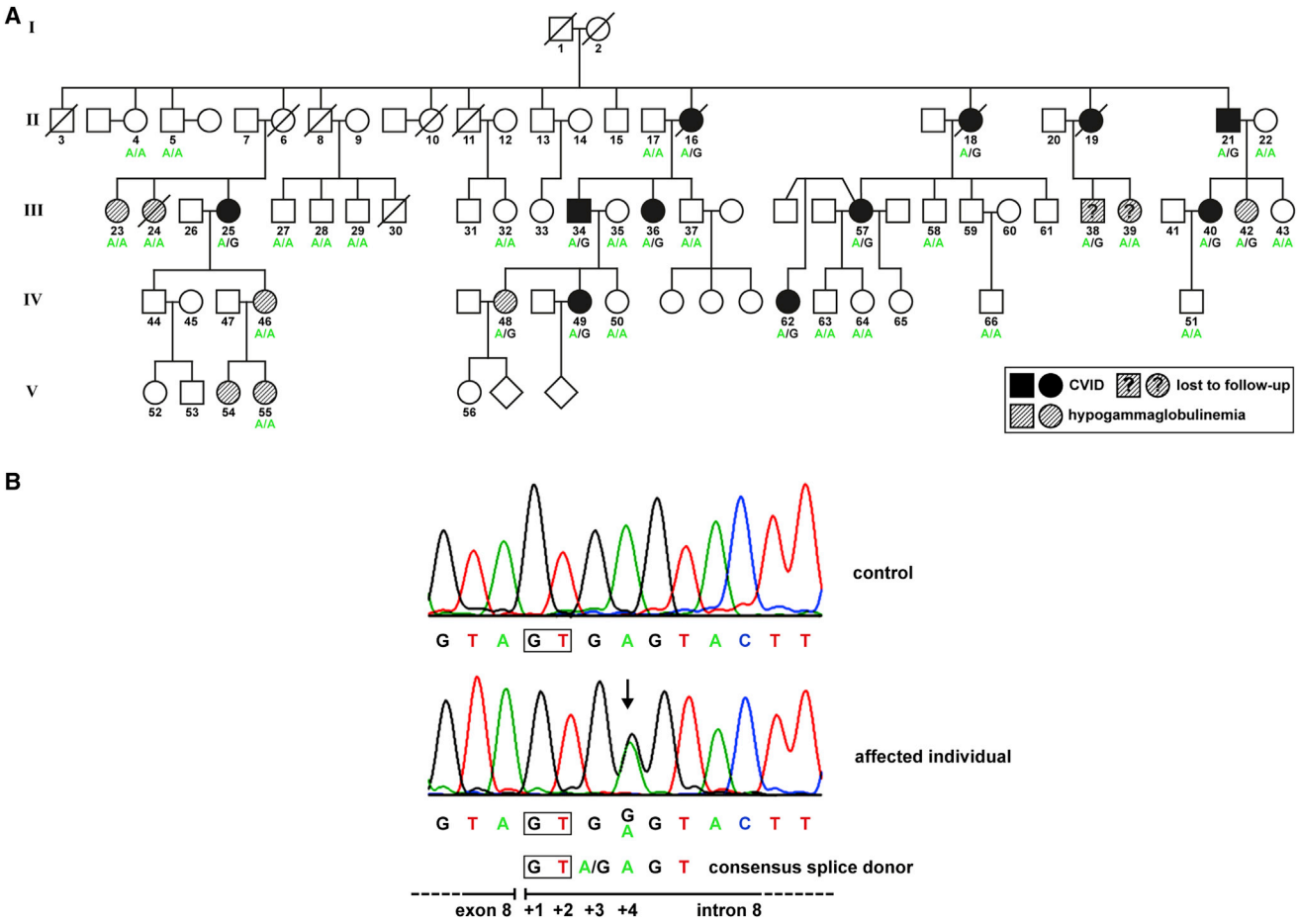

Figure 1. Autosomal-Dominant Inheritance of a Heterozygous *NFKB1* Mutation in a Large CVID-Affected Family
(A) The pedigree of FamNL1[52] was completed and revised after re-evaluation of clinical records and follow-up examinations. Circles, female; squares, male; filled symbols, affected individual with CVID; hatched symbols, affected individual with hypogammaglobulinemia; open symbol, healthy member with wild-type *NFKB1*; slash, deceased individual.
(B) The mutation (c.730+4A>G) affects the intron 8 splice donor site, which perfectly aligns to the consensus splice site.

and FamNL1-48) harbored the mutation (Figure 1A). An inconsistency was observed in one individual with an ambiguous medical history (FamNL1-39) who does not carry the mutation and who was hence classified as a "phenocopy." The presence of a phenocopy is not surprising in light of the high incidence of hypogammaglobulinemia in this family. The possibilities of phenocopies and non-penetrance have been included in the previous genetic linkage analysis.[52] In four of the tested individuals with hypogammaglobulinemia (FamNL1-23, FamNL1-24, FamNL1-46, and FamNL1-55,), the mutation was also undetectable. These family members are together on one branch of the pedigree, suggesting the presence of other genetic factors associated with hypogammaglobulinemia in this branch.

The *NFKB1* Intron 8 Splice-Donor-Site Mutation Causes In-Frame Skipping of Exon 8

Because the identified sequence variant c.730+4A>G affects the splice donor site of intron 8, we next tested whether NF-κB1 mRNA splicing was affected. We analyzed the mRNA expression in EBV-transformed B lymphocytes derived from affected individuals (n = 3) and a healthy control individual by RT-PCR (Figure 2A). Using primers spanning exons 7 to 10, we observed a single band with the expected size; this band was in the control sample. In contrast, in samples from affected individuals, an additional shorter product was obtained, indicating skipping or mis-splicing of either exon 7, 8, or 9.

In the control sample, sequencing of the cDNA product was normal. In contrast, the shortened product in the mutant samples lacked exon 8 (159 bp). Thus, the mutation of the splice donor site in intron 8 most likely renders exon 8 unrecognizable to the splicing machinery and thus causes in-frame splicing of exon 7 to exon 9 (Figure 2B).

A Deletion within the NF-κB1 RHD in p105ΔEx8 Leads to Rapid Degradation and p50 Haploinsufficiency

As a consequence of the *NFKB1* splice-donor-site mutation, in-frame skipping of exon 8 predicts the deletion of an internal 53-amino-acid fragment from the N-terminal RHD with insertion of a glutamic acid residue due to the fusion

Table 1. Clinical Information of 20 Individuals Harboring *NFKB1* Mutant Alleles

Individual	Year of Birth	Year of Diagnosis	Diagnosis	IgG (g/L)	IgA (g/L)	IgM (g/L)	Clinical Phenotype
FamNL1							
16	1935	1964	CVID	2.76	0.30	0.16	COPD, pyoderma gangrenosum, pansinusitis, atrophic gastritis, squamous cell carcinoma, respiratory tract infections, pneumonia; died due to pulmonary insufficiency
18	1936	2000	CVID	2.49	0.13	0.53	sinopulmonary infections, splenomegaly, lymphadenopathy, mild thrombocytopenia, ischemic heart disease, lung adenocarcinoma
21	1940	1997 (2000)[a]	CVID	6.0	1.26 (0.93)[a]	0.4 (0.17)[a]	COPD, pneumonia, recurrent sinusitis, bronchiectasis, lung fibrosis, respiratory insufficiency
25	1948	uk	CVID	4.6	1.0	0.4	COPD, pulmonary infections, respiratory insufficiency, cor pulmonale
34	1960	uk	CVID	8.0	0.83	0.25	autoimmune hypothyroidism, alopecia areata, recurrent respiratory infections, pyoderma gangrenosum
36	1961	1991	CVID	1.81	0.06	0.48	recurrent sinusitis, pneumonia
40	1966	uk	CVID	5.1	<0.5	0.65	COPD, recurrent upper airway infections
42	1968	uk	HGG	uk	uk	uk	recurrent paronychia and superficial skin infections, minor laboratory abnormalities
48	1985	uk	HGG	3.72	0.59	0.74	aortic stenosis, furunculosis, folliculitis, autoimmune thyroiditis
49	1986	1988	CVID	9.1[b]	1.41	0.11	enteritis, recurrent otitis media, giardiasis, recurrent respiratory infections
57	1961	2000	CVID	1.3	<0.04	0.3	LIP, NRH, recurrent sinopulmonary infections
62	1985	2015	CVID	4.7	0.4	0.3	mild recurrent sinus infections
Fam089							
II1	1946	2010	CVID	1.42	0.08	0.4	severe pneumonia, pleural empyema, multiple liver hemangiomas
II2	1979	1995 (2006)[a]	CVID	6.29 (4.41)[a]	<0.3 (<0.07)	<0.3 (0.2)[a]	ITP, recurrent pulmonary infections, autoimmune hemolytic anemia, hepatomegaly, lymphadenopathy
III2	2009	2014	HGG	1.94	<0.07	0.29	transient HGG
III4	2013	–	–	–	–	–	healthy
FamNZ							
I2	1941	–	–	9.9	0.58	0.8	alopecia, thrombocytopenia, normal immunoglobulins
II1	1966	1968	CVID	5.17	0.07	0.5	thrombocytopenia, neutropenia, autoimmune hemolytic anemia
II2	1968	1988	CVID	–	–	–	alopecia, bronchiectasis, NRH, marginal-zone non-Hodgkin lymphoma
II3	1971	–	–	7.78	1.5	0.56	healthy

CVID, common variable immunodeficiency; HGG, hypogammaglobulinemia; COPD, chronic obstructive pulmonary disease; LIP, lymphocytic interstitial pneumonitis; NRH, nodular regenerative hyperplasia; ITP, idiopathic thrombocytopenic purpura; uk, unknown.
[a]Additional data from follow-up exam.
[b]IgG levels after IVIG.

of exons 7 and 9 (p.Asp191_Lys244delinsGlu). Because p105 is processed to p50 by limited proteolysis of its C-terminal half, the deletion is predicted to affect both the precursor and mature NF-κB1 proteins (Figure S1).

To test whether a shortened protein (with a molecular weight reduced by ~5.8 kDa) is produced from the mutant mRNA, we analyzed protein extracts from EBV B cell lines from affected individuals (n = 3), healthy family members (n = 3), and healthy control individuals (n = 2) by western blotting. Using an antibody raised against the N-terminal end of NF-κB1, we detected both subunits p105 and p50 in crude lysates in all analyzed samples (Figure 2C). Yet, in the heterozygous affected individuals, both p105 and p50 protein amounts were uniformly lower (reduced to ~50%) than those in non-affected family members and control individuals, consistent with expression exclusively from the non-mutant allele. As predicted, a smaller additional band was detected in all samples from affected

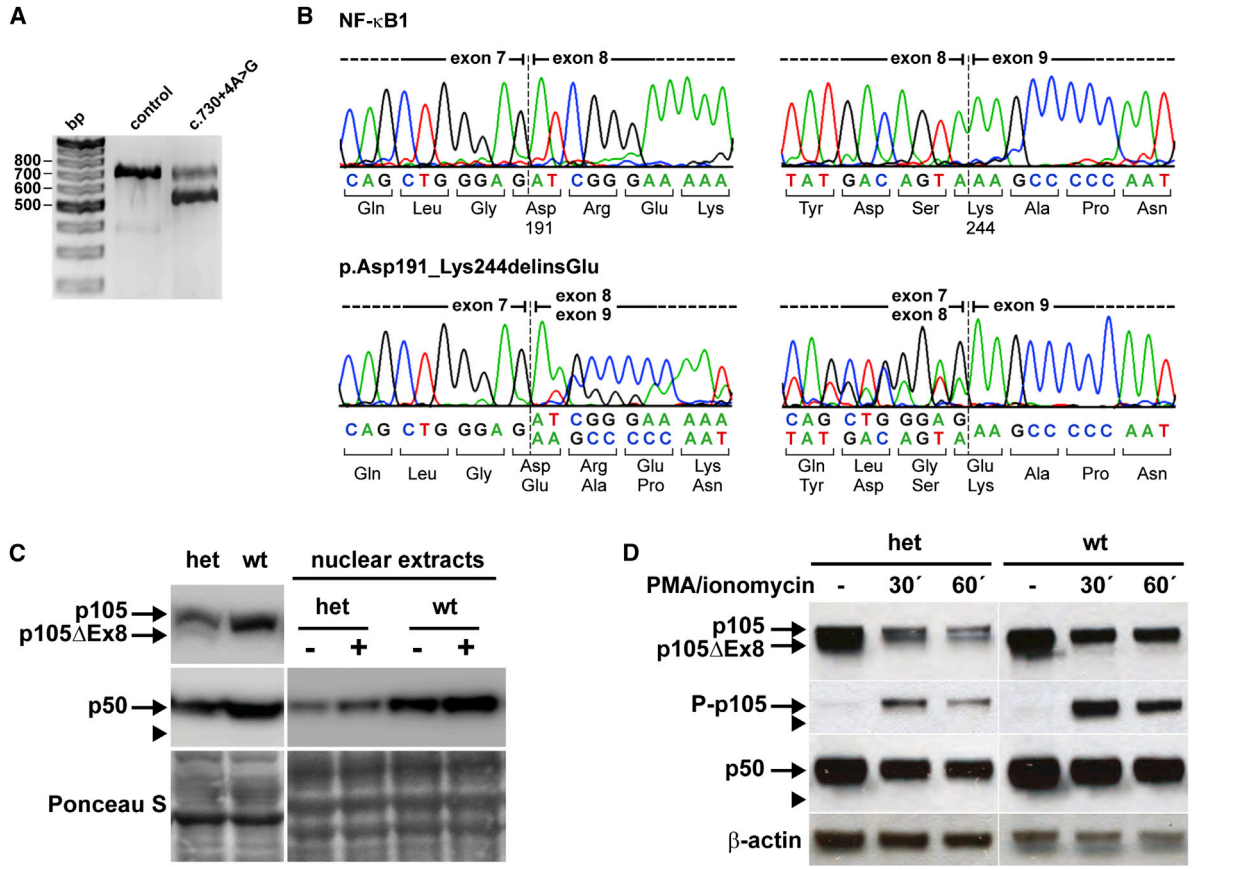

Figure 2. The Heterozygous Splice-Donor-Site Mutation in Intron 8 of *NFKB1* Causes In-Frame Skipping of Exon 8 and Haploinsufficiency of the p50 Subunit

(A) EBV-transformed B cell lines derived from a healthy control individual and affected individuals (n = 3) were analyzed by RT-PCR for correct *NFKB1* mRNA splicing with primers located in exons 6 and 11. In addition to the expected band (649 bp) a shorter product is observed in affected individuals, which indicates the loss of either exon 7 (164 bp), 8 (159 bp), or 9 (105 bp). Representative results are shown.

(B) Sequencing of the RT-PCR products shows normal splicing in the control individual (upper panels). The heterozygous mutation (c.730+4A>G) causes skipping of exon 8 and in-frame fusion of exon 7 to exon 9 (lower panels: left, forward; right, reverse), indicated by the double peaks at the exon borders. The mutant mRNA predicts the translation of a shortened NF-κB1 p105 (p105ΔEx8) with a 53-amino-acid internal deletion (p.Asp191_Lys244delinsGlu).

(C) EBV B cell lines from affected persons (n = 3) harboring the heterozygous *NFKB1* mutation (het), from unaffected (wt) family members (n = 4) and healthy control cells (n = 2) were stimulated with PMA plus ionomycin as indicated (−/+) and analyzed by western blot for NF-κB1 protein amounts with antibodies raised against the N terminus of both p150 and the processed form, p50. Representative results are shown. As depicted in the left panel, the altered protein p105ΔEx8 is only marginally preserved and processing to p50ΔEx8 is not detectable (expected size is indicated by the arrowhead). Overall amounts of both p105 and p50 are reduced to ~50% in EBV B cells from affected individuals (het). As depicted in the right panel, activation and nuclear translocation of residual p50 (derived only from the non-mutant allele) in affected individuals and normal nuclear translocation of p50 in controls after PMA plus ionomycin stimulation for 45 min. Ponceau S staining was used to demonstrate equal loading.

(D) PBMCs from affected family members (n = 2) and healthy control individuals (n = 4) were stimulated with PMA plus ionomycin as indicated, and cell lysates were analyzed for p105 and p50 amounts and for phosphorylation of p105 (Ser933, P-p105) by western blotting (representative results). In samples derived from affected individuals, both p105 and the altered p105ΔEx8 are detectable. Only the non-altered p105 is phosphorylated. Phosphorylation of p105ΔEx8 and processing to p50ΔEx8 is undetectable (arrowheads). Whether stimulated or not, p50 is sustained at reduced amounts in comparison to that in controls. β-actin was used as a loading control.

individuals. The molecular weight of this protein corresponds to the truncated p105, which is translated from the mutant allele and lacks the sequences encoded by exon 8 (p105ΔEx8). Unexpectedly, however, the altered protein band was evidently less intense than its wild-type counterpart.

The marginal abundance of p105ΔEx8 indicated that the mutant mRNA or altered protein was either only weakly transcribed or translated, respectively, or rapidly degraded. Most importantly, an additional smaller band corresponding to p50ΔEx8 (~44 kDa) was never detected. Thus, in contrast to p105, which was processed to the active p50 subunit, the mutant p105ΔEx8 was not processed to a corresponding truncated form (p50ΔEx8). We concluded that, in EBV B cell lines from affected individuals, the amount of p105ΔEx8 is not sustained, and instead, the altered protein is rapidly degraded. The p105 and p50 proteins, translated from the non-mutated allele, are normal.

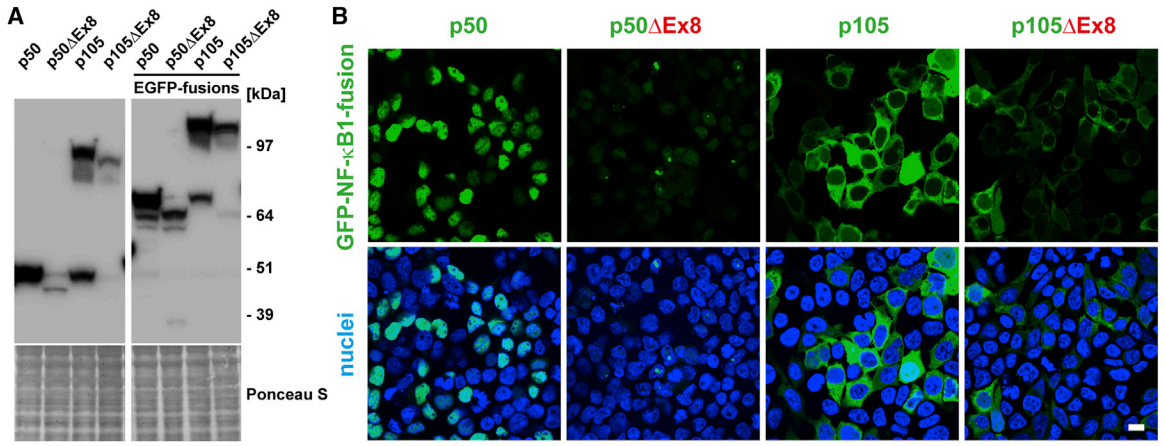

Figure 3. Rapid Elimination of Altered p50ΔEx8 and p105ΔEx8 in Transfected Cells
(A) HEK293T cells were transiently transfected with the indicated constructs, and the amounts of the ectopic proteins were analyzed in crude lysates by western blot. The altered proteins gain only weak signals and processing of p105ΔEx8 to p50ΔEx8 is almost undetectable. The faint band at 50 kDa in all lanes is the endogeneous p50. Molecular weight markers are indicated on the right side. Ponceau S staining of the blotting membranes confirm equal loading.
(B) Fluorescence imaging shows nuclear localization of GFP-p50 and cytoplasmic localization of GFP-p105. Only aberrant signals are detected with the mutant proteins. Green, GFP-fusion proteins as indicated; blue, nuclei. Scale bar represents 10 μm.

The internal deletion is predicted to affect the RHD, which mediates dimerization, nuclear translocation, and DNA binding. Thus, the altered proteins (p105ΔEx8 and/or p50ΔEx8) potentially could interfere with NF-κB1-mediated signaling. We wanted to confirm that no mutant p50ΔEx8, although undetectable in crude lysates, is translocated to the nucleus after NF-κB pathway stimulation. We therefore treated EBV-transformed B cells derived from affected individuals (n = 3), unaffected family members who do not carry the mutation (n = 4), and healthy control individuals (n = 2) with non-specific NF-κB1 activators (PMA plus ionomycin) and analyzed the amount of p50 translocation in nuclear protein extracts (Figure 2C). In western blot analyses, the "active" nuclear p50 was also detected only at severely reduced amounts in unstimulated samples derived from affected individuals in comparison to levels in control samples. After stimulation, p50 was increased in samples from affected individuals but only reached approximately half the amount observed in the control individuals. Again, the hypothetical altered form, p50ΔEx8, was not detected.

These findings were further confirmed by western blot analysis of lysates from PBMCs isolated from affected family members and healthy control individuals (Figure 2D). In the samples from affected family members, the precursors produced from both the wild-type allele (p105) and the mutant allele (p105ΔEx8) were detectable. Upon stimulation of the cells with PMA plus ionomycin, only the wild-type p105 was phosphorylated (Ser933). Thus, the total amount of phosphorylated p105 (phospho-p105) was reduced to ~50% of the amount seen in control samples. Consistently, only the wild-type p105 was further processed to p50, whereas processing of p105ΔEx8 to a mutant p50ΔEx8 was not detectable. Similar results were obtained when cells were treated with CD40L (data not shown).

In summary, these observations suggest that the heterozygous c.730+4A>G splice-donor-site mutation leads to rapid degradation of an aberrant protein, p105ΔEx8, which is not further processed to p50ΔEx8 and thus causes a functional haploinsufficiency of NF-κB1 subunit p50.

Rapid Elimination of Altered p50ΔEx8 and p105ΔEx8 in Transfected Cells

To verify that the existence of both the p105ΔEx8 and hypothetical p50ΔEx8 proteins are not tolerated in viable cells and thus are degraded, we generated cytomegalovirus promoter-driven vectors for ectopic expression in cell-culture models. We transiently transfected p50, p50ΔEx8, p105, and p105ΔEx8, as well as N-terminal GFP-fusion constructs (GFP-p50 and GFP-p50ΔEx8, GFP-p105 and GFP-p105ΔEx8), in human embryonic kidney cells (HEK293T) and/or murine NIH 3T3 fibroblasts (Figure 3 and data not shown). Western blot analyses showed that the non-mutant proteins p50 and p105, as well as their GFP-fused derivatives, were highly abundant upon transient transfection. In contrast, the protein amounts of the truncated p50ΔEx8 and p105ΔEx8 were only modest, whether fused to GFP or not (Figure 3A). Furthermore, both ectopic p105 variants were readily processed to p50 and GFP-p50, respectively, whereas proteolytically produced p50ΔEx8 and GFP-p50ΔEx8 were almost undetectable (Figure 3A).

Consistently, confocal fluorescence microscopy demonstrated that GFP-p50 localized to the nucleus in transfected cells, whereas GFP-p50ΔEx8 showed only speckled fluorescence signals in individual cells (Figure 3B). In contrast to transiently transfected GFP-p105, which was detected at high levels, mainly within the cytoplasm, only very weak GFP-p105ΔEx8 signals were detected. These observations indicate that the altered proteins (p105ΔEx8 and

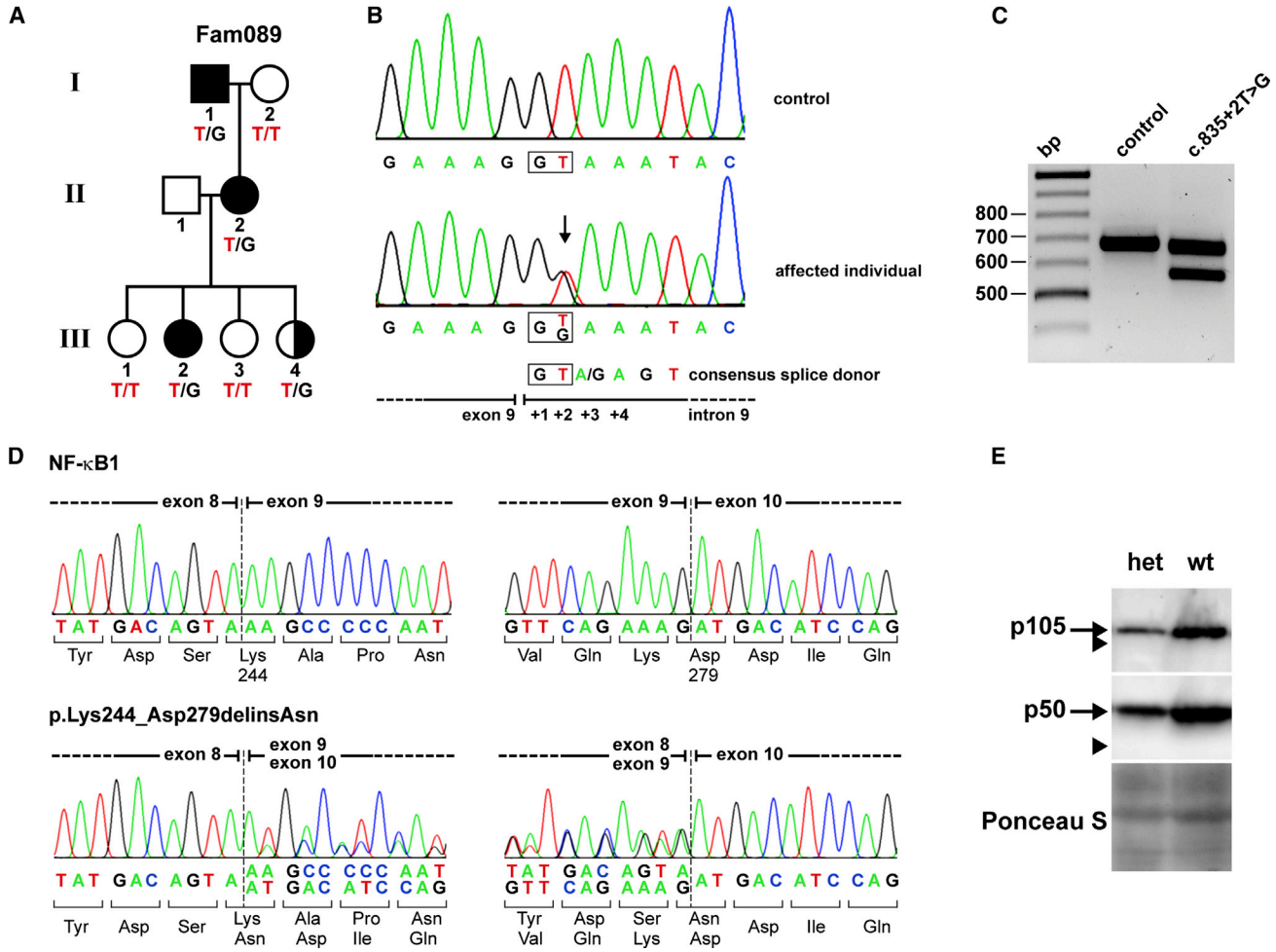

Figure 4. Haploinsufficiency of p50 Due to a Heterozygous Splice-Donor-Site Mutation in Intron 9 of *NFKB1*
(A) Autosomal-dominant inheritance of a heterozygous *NFKB1* mutation in family Fam089. Shaded symbols, affected members; half-shaded symbol, healthy members harboring the mutation.
(B) The mutation (c.835+2T>G) affects the splice-donor-site mutation in intron 9.
(C) RT-PCR shows an additional shorter band in EBV-transformed B cells from the proband, indicating exon skipping.
(D) cDNA sequencing demonstrates skipping of exon 9. In-frame fusion of exon 8 to exon 10 predicts a shortened NF-κB1 p105 (p105ΔEx9) with a 35-amino-acid internal deletion (p.Lys244_Asp279delinsAsn).
(E) Western blotting shows reduced amounts of p105 and p50 in EBV B cell lines from affected individuals (n = 2) in comparison to those in unaffected family members (n = 2) and healthy control cells (n = 2). The predicted altered proteins p105ΔEx9 and p50ΔEx9 are undetectable (arrowheads), indicating rapid elimination or mRNA decay. Representative results are shown.

p50ΔEx8) are highly unstable and probably non-functional, thus allowing NF-κB1-mediated transcriptional activation (via p105 and p50, translated from the non-mutant allele) to be sustained.

Identification of a Splice-Donor-Site Mutation in Intron 9 of *NFKB1* by Targeted NGS in a German CVID-Affected Family

To identify disease-causing mutations in a cohort of CVID-affected families, we screened candidate genes, including *NFKB1*, by targeted NGS. In one family, Fam089 (Figure 4A), we identified a second heterozygous splice-donor-site mutation (Figure 4B). In contrast to the mutation in FamNL1, this mutation affected intron 9 (c.835+2T>G [GenBank: NM_003998.3]). This sequence variant caused in-frame skipping of exon 9 (Figures 4C and 4D) and also resulted in haploinsufficiency of p50 (Figure 4E). Variant p50ΔEx9 (p.Lys244_Asp279delinsAsn) was not detected (Figure 4E and Figure S1).

Identification of a Frameshift Mutation in *NFKB1* by WES in a CVID-Affected Family from New Zealand

To identify the disease-causing mutation in a family from New Zealand with European descent (FamNZ; Figure 5A), genomic DNA was isolated from PBMCs of the male proband (FamNZ-II1), his mother (FamNZ- I2), and his affected sister (FamNZ-II2). Samples were then subjected to WES. We identified a total of 79 variants that were shared between the three sequenced exomes and which are rare in the European population (allele frequency ≤ 0.02), and are likely to affect the protein function. One of these variants was a *NFKB1* heterozygous frameshift

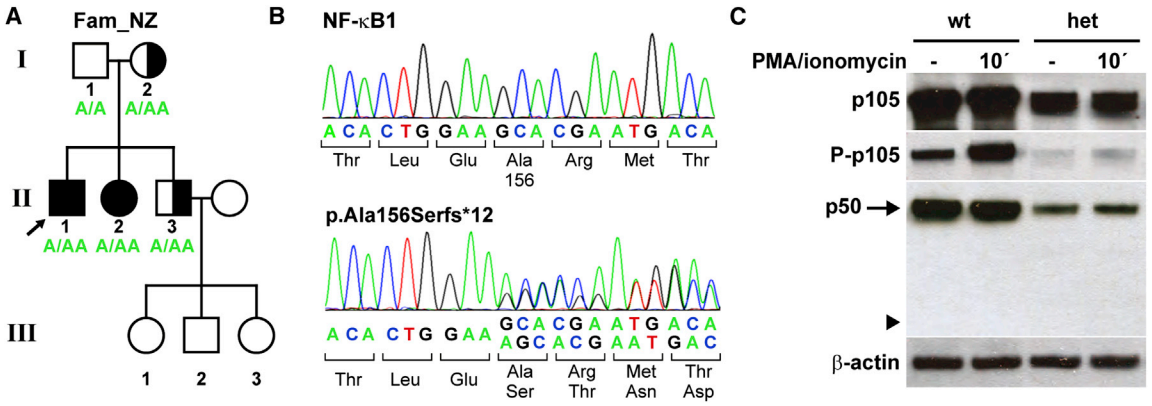

Figure 5. A Frameshift Mutation in *NFKB1* Causes p50 Haploinsufficiency in a CVID-Affected Family from New Zealand
(A) A heterozygous one-base-pair duplication (c.465dupA) in exon 7 was identified in the indicated family members. The three children in the third generation were not tested. Shaded symbols, affected members; half-shaded symbols, healthy members harboring the mutation.
(B) The single-base-pair insertion predicts a shift of the reading frame and the premature termination of translation (p.Ala156Serfs*12).
(C) PBMCs from affected family members (n = 3) and healthy control individuals (n = 3) were stimulated with PMA plus ionomycin as indicated and analyzed by western blotting. Representative results are shown. In affected individuals, normal p105 can only be derived from the healthy allele. Thus, p105 amounts, phosphorylation of p105, and processing to p50 are severely reduced in comparison to controls. The mutation predicts the translation of a non-functional severely truncated protein (~18 kDa in size), which is not detectable (arrowhead). The β-actin control confirms equal loading.

mutation, which was confirmed by Sanger sequencing in the proband, his mother, and his siblings (Figures 5A and 5B). The one base-pair duplication (c.465dupA [GenBank: NM_003998.3]) in exon 7 causes a premature termination of translation and predicts the translation of a non-functional, severely truncated protein (p.Ala156Serfs*12, ~18 kDa) that retains only the N-terminal part of the RHD and lacks all other functional domains (Figure S1B). This variant is absent from the 61,000 exomes of the Exome Aggregation Consortium cohorts and has not been reported previously.

To test whether a truncated 166-amino-acid protein is produced from the mutant allele, we analyzed PBMCs from affected family members and healthy control individuals by western blotting (Figure 5C). In heterozygous affected individuals, overall amounts and phosphorylation of p105, as well as p50 amounts, were severely reduced in comparison to those in the control individuals. Phospho-p105 was increased following activation of NF-κB-signaling in these cells, indicating that residual p105 translated from the non-mutant allele was normal. However, when we used the antibodies directed against the N-terminal amino acids, no truncated protein was detectable. Hence, it appears unlikely that NF-κB1-dependent signaling can be impaired by the presence of a remnant protein. We therefore conclude that, in the CVID-affected family FamNZ, the heterozygous c.465dupA mutation in *NFKB1* also causes a functional p50 haploinsufficiency.

Discussion

In this study, we demonstrated that two heterozygous splice-site mutations and a frameshift mutation affecting the RHD of *NFKB1* are associated with CVID in three unrelated families from diverse geographical regions. The mutations cause in-frame skipping of exon 8 or exon 9 or premature termination of translation, respectively. In each case, the altered protein (p105ΔEx8; p105ΔEx9, p.Ala156Serfs*12) is rapidly degraded, and no further processing to the truncated active protein (p50ΔEx8 or p50ΔEx9) occurs. Because p105 and p50 translated from the non-mutant alleles were apparently normal in all three pedigrees (with an overall amount of ~50% of that in healthy control individuals), we concluded that NF-κB1 haploinsufficiency accounts for the CVID phenotypes in the affected family members.

Maintenance of Residual NF-κB1 Function through Decay of the Altered Proteins

The in-frame deletions of either amino-acid residues 191–244 (corresponding to exon 8) or of amino-acid residues 244–279 (corresponding to exon 9) partially delete the N-terminal RHD (Figure S1B). Conversely, the C-terminal portion of p105, which determines the processing to p50 (via phosphorylation at S928 and S933, subsequent poly-ubiquitination at multiple sites, and proteasomal cleavage at amino-acid 433), is not affected by these mutations.

Because in-frame skipping can theoretically lead to aberrant proteins, we initially expected that the altered proteins p50ΔEx8 and p50ΔEx9 would be detectable in affected individuals and would interfere with NF-κB1-mediated signaling by impairing homo- or heterodimerization, nuclear translocation, and/or DNA binding. It is also conceivable that the altered p105ΔEx8 and p105ΔEx9 block the proteasome, causing false or delayed processing of p105 translated from the non-mutant allele, and thus exert a dominant negative effect on NF-κB1-mediated signaling. In contradiction to both hypotheses, we never

detected p50ΔEx8 or p50ΔEx9 in primary cells or EBV-transformed B lymphocytes derived from affected individuals by western blotting (Figures 2C and 2D) and only marginal amounts after forced transient transfection of p105ΔEx8 or even p50ΔEx8 in HEK293T cells (Figure 3A). Remarkably, fusion of GFP to their N termini did not substantially stabilize the altered p105ΔEx8 or p50ΔEx8 and only slightly delayed their degradation (Figures 3A and 3B). These observations are consistent with a previous report, demonstrating that an internal-deletion variant, p105Δ(356–498), was completely degraded by the 20S proteasome in vitro,[58] whereas deletion of the N-terminal 1–245 amino acids of p105 had no effect on p50 processing. Thus, the presence of mutant p105ΔEx8 or p105ΔEx9, which both undergo rapid protein decay, is most likely irrelevant to the disease etiology. This observation is supported by the third *NFKB1* mutation identified in this study. The frameshift mutation c.465dupA, if translated, would yield a 166-amino-acid protein (p.Ala156Serfs*12; including the N-terminal 155-amino-acid residues of p105 and p50, plus 11 amino acids encoded by the frameshifted sequence). However, no evidence was found for persistent amounts of a remnant protein.

Our results further suggest that NF-κB1 amounts are tightly regulated, and the heterozygous loss of p50 cannot be balanced, e.g., through increased expression from the non-mutant allele. It remains to be tested whether the ratio of cytoplasmic versus nuclear p50-RelA, before and after pathway stimulation, is also abnormal in cells derived from affected individuals. Such analyses (e.g., by methods based on confocal imaging) might be useful in future routine screenings of immunodeficiencies with NF-κB1 haploinsufficiency.

A functional haploinsufficiency of NF-κB1 p50 associated with immunodeficiency has also been reported in affected individuals with mutations in *NFKBIA* (*IKBA*).[59] In addition, NFKB2 haploinsufficiency has been acknowledged as the disease-causing mechanism of CVID-associated *NFKB2* mutations.[46–51] Furthermore, several reports have supported a functional haploinsufficiency as the predominant disease mechanism associated with various primary immunodeficiencies and autoimmune phenotypes caused by mutations in *TACI*,[60,61] *CTLA4*,[15,62] *NFAT5*[63] (MIM: 04708), *VAV1*[64] (MIM: 164875), *GATA2*[65] (MIM: 137295), and others. Thus haploinsufficiency, frequently associated with incomplete penetrance, appears as a recurrent paradigm and emphasizes the requirement for accurate gene regulation within the immune system.[66]

Other Possible Splicing Errors

The consensus splice donor site (see Figure 1B) predicts frequencies of 100% for both the guanine and the thymidine at the positions +1 and +2, respectively, but only of 70% for an adenine at position +4. Thus, the mutation c.835+2T>G in Fam089 probably completely inactivates the splice donor site in intron 9, whereas the mutant allele in FamNL1 (c.730+4A>G) could potentially retain residual splice-donor function. We cannot exclude, though, that alternative splice sites are used instead of the mutant sites or that other errors occur, thereby leaving the intron or parts thereof un-spliced. Accordingly, weak bands with aberrantly increased sizes were detectable under certain RT-PCR conditions (data not shown). However, these have not been further investigated because additional aberrant proteins have not been observed.

Variable Clinical Phenotype of CVID-Affected Individuals with p50 Haploinsufficiency

In addition to the adaptive immune response, the canonical NF-κB pathway plays many essential roles in innate immune responses such as toll-like receptor (TLR)-mediated signaling, cytokine production in response to microbial stimulation, and inflammatory responses. Upon initiation of the canonical NF-κB cascade, NEMO-containing IKK complexes lead to degradation of IκBα and release of NF-κB dimers. Thus, defects in NF-κB1 would also be expected to impair innate immune functions and, for instance, cause increased susceptibility to skin or airway infections. Conversely, individuals affected with innate immune system defects mostly have intact adaptive immune systems with normal B- and T-cell function and antibody amounts. The affected family members in our study were initially diagnosed with CVID, mainly based on laboratory findings, commonly with low immunoglobulin levels. Phenotypic observations of these family members were variable, comprising an increased susceptibility to infections, skin lesions, lymphoma, and inflammatory bowel disease. However, characteristic defects of the innate immune system were not directly obvious. Similarly, mutations in upstream components of NF-κB1, such as *TLR3* (MIM: 603029), *MYD88* (MIM: 602170), *IRAK4* (MIM: 606883), *HOIL1* (MIM: 610924), *IKBKG (NEMO)*, and *NFKBIA (IKBA)*, all lead to specific defects of the innate immune system.[67] A possible NF-κB1 dosage effect due to a promoter polymorphism might be associated with ulcerative colitis, given that reporter constructs with the −94delATTG allele showed less activity than constructs with the −94insATTG allele.[41] Thus, although variable, NF-κB1 p50 haploinsufficiency characterizes a unique disease entity.

Both, the Dutch-Australian family and the German family showed a highly variable age of onset of the CVID phenotype. For instance, individuals 18 and 21 in FamNL1 were only diagnosed at ages 65 and 57, respectively, whereas individual 62 in FamNL1 appears to be developing progressing CVID symptoms at the age of 30 years. She was diagnosed with CVID on the basis of the genetic result of the current study and is not yet on intravenous immunoglobulin (IVIG) replacement therapy. Similarly, individual I1 in Fam089 has only now been diagnosed with CVID at the age of 64 years. In contrast, individuals 49 from FamNL1 and II2 from Fam089 both presented with initial symptoms in early childhood. Additionally, the severity of

the disease varies considerably between individual members of each family. II2 from Fam089 shows a profound CVID phenotype associated with lymphoproliferation, lung disease, autoimmune cytopenias, and enteropathy, whereas her father (Fam089-I1) has an infection-only disease phenotype. In this family, the youngest family member, (Fam089-III4, 2 years of age) also harbors the mutation and has not developed any signs of disease to date but could develop disease later in her life. However, the penetrance of the various disease phenotypes at the different decades of life is currently not known.

In the New Zealand family, the heterozygous frameshift mutation c.465dupA is also associated with highly divergent disease phenotypes varying from asymptomatic to severe manifestations with malignancy and autoimmunity in addition to bronchiectasis. The reasons for the phenotypic variations, as well as for the variable age of disease onset, associated with p50 haploinsufficiency in this family remain speculative. It is possible that modifier genes, which are yet to be identified, account for the observed variability of penetrance and expressivity. Remarkably, both affected female members of this family, as well as the affected individual 34 in FamNL1, have alopecia, a phenotypic observation that has previously been associated with mutations in *NFKB2* (MIM: 164012).[48] However, we did not find evidence for additional mutations in other genes implicated in CVID when analyzing the index subjects by WES or NGS.

Abnormal B Cell Physiology in *Nfkb1*-Deficient Mice

Nfkb1$^{-/-}$ mice, which lack the homologous p50 subunit of NF-κB1, exhibit no developmental or lethal abnormalities and reproduce normally.[68] However, they show multifocal defects in immune responses involving B lymphocytes and nonspecific responses to infection. B cell dysfunction in these mice includes decreased proliferation, abnormal class-switch recombination, decreased marginal-zone B cell numbers, abnormal humoral immune response, and decreased immunoglobulin levels, with defective basal and specific antibody production.[21,22,60] Their phenotypic abnormalities also include increased susceptibility to infection with *S. pneumoniae*, large intestinal inflammation, abnormal CD4-positive T cell physiology, and abnormal secretion of cytokines. Interestingly, late-onset alopecia has recently been reported in *Nfkb1*$^{-/-}$ mice,[69] similar to the phenotype observed in FamNZ and FamNL1 in this study. With regard to the disease symptoms in CVID-affected persons with *NFKB1* mutations, analyzing the effects of p50 haploinsufficiency in *Nfkb1*$^{+/-}$ mice will be an interesting task of future investigation.

In this study, we employed NGS technologies to identify three distinct mutations in *NFKB1* in three CVID-affected families. The identification of mutations in this central regulator of inducible gene expression in the immune system could advance our understanding of the molecular pathomechanisms that lead to primary immunodeficiencies.

Supplemental Data

Supplemental Data include case reports and one figure and can be found with this article online at http://dx.doi.org/10.1016/j.ajhg.2015.07.008.

Acknowledgments

We are deeply grateful to all the affected individuals and their families who participated in this study. We thank Mary Buchta, Franziska Nussbaumer, Pavla Mrovecova, Katrin Hübscher, Tobias Kratina, and Isabella Kong for their excellent technical assistance. We thank Marcel van Deuren for sharing clinical data on the Dutch family. This study was supported by the German Federal Ministry of Education and Research (01EO1303), E:med SysINFLAME Collaborative Project 1 (01ZX1306), the Australian National Health and Medical Research Council (1054925) and the Auckland Medical Research Foundation, the Auckland District Health Board Charitable Trust, and the New Zealand eScience Infrastructure. This work was supported in part by the Intramural Research Program of the NIH, National Library of Medicine. C.S. was supported by National Health and Medical Research Council postgraduate scholarship 1075666.

Received: June 1, 2015
Accepted: July 16, 2015
Published: August 13, 2015

Web Resources

The URLs for data presented herein are as follows:

1000 Genomes, http://www.1000genomes.org/
Burrows-Wheeler Aligner, http://bio-bwa.sourceforge.net
Ensembl Genome Browser, http://www.ensembl.org/index.html
ExAC Browser, http://exac.broadinstitute.org/
IGV, http://www.broadinstitute.org/igv/
NF-κB target genes, www.bu.edu/nf-kb/gene-resources/target-genes
OMIM, http://www.omim.org/
Picard, http://broadinstitute.github.io/picard
RefSeq, http://www.ncbi.nlm.nih.gov/RefSeq

References

1. Cunningham-Rundles, C. (2012). The many faces of common variable immunodeficiency. Hematology (Am Soc Hematol Educ Program) *2012*, 301–305.
2. Ameratunga, R., Brewerton, M., Slade, C., Jordan, A., Gillis, D., Steele, R., Koopmans, W., and Woon, S.T. (2014). Comparison of diagnostic criteria for common variable immunodeficiency disorder. Front. Immunol. *5*, 415.
3. Yong, P.F., Thaventhiran, J.E., and Grimbacher, B. (2011). "A rose is a rose is a rose," but CVID is Not CVID common variable immune deficiency (CVID), what do we know in 2011? Adv. Immunol. *111*, 47–107.
4. Hammarström, L., Vorechovsky, I., and Webster, D. (2000). Selective IgA deficiency (SIgAD) and common variable immunodeficiency (CVID). Clin. Exp. Immunol. *120*, 225–231.
5. Cunningham-Rundles, C., and Bodian, C. (1999). Common variable immunodeficiency: clinical and immunological features of 248 patients. Clin. Immunol. *92*, 34–48.

6. Vorechovský, I., Zetterquist, H., Paganelli, R., Koskinen, S., Webster, A.D., Björkander, J., Smith, C.I., and Hammarström, L. (1995). Family and linkage study of selective IgA deficiency and common variable immunodeficiency. Clin. Immunol. Immunopathol. *77*, 185–192.
7. Aghamohammadi, A., Mohammadi, J., Parvaneh, N., Rezaei, N., Moin, M., Espanol, T., and Hammarstrom, L. (2008). Progression of selective IgA deficiency to common variable immunodeficiency. Int. Arch. Allergy Immunol. *147*, 87–92.
8. Johnson, M.L., Keeton, L.G., Zhu, Z.B., Volanakis, J.E., Cooper, M.D., and Schroeder, H.W., Jr. (1997). Age-related changes in serum immunoglobulins in patients with familial IgA deficiency and common variable immunodeficiency (CVID). Clin. Exp. Immunol. *108*, 477–483.
9. Español, T., Catala, M., Hernandez, M., Caragol, I., and Bertran, J.M. (1996). Development of a common variable immunodeficiency in IgA-deficient patients. Clin. Immunol. Immunopathol. *80*, 333–335.
10. Ameratunga, R., Woon, S.T., Gillis, D., Koopmans, W., and Steele, R. (2013). New diagnostic criteria for common variable immune deficiency (CVID), which may assist with decisions to treat with intravenous or subcutaneous immunoglobulin. Clin. Exp. Immunol. *174*, 203–211.
11. Driessen, G., and van der Burg, M. (2011). Educational paper: primary antibody deficiencies. Eur. J. Pediatr. *170*, 693–702.
12. Warnatz, K., Denz, A., Dräger, R., Braun, M., Groth, C., Wolff-Vorbeck, G., Eibel, H., Schlesier, M., and Peter, H.H. (2002). Severe deficiency of switched memory B cells (CD27(+)IgM(-)IgD(-)) in subgroups of patients with common variable immunodeficiency: a new approach to classify a heterogeneous disease. Blood *99*, 1544–1551.
13. Horn, J., Manguiat, A., Berglund, L.J., Knerr, V., Tahami, F., Grimbacher, B., and Fulcher, D.A. (2009). Decrease in phenotypic regulatory T cells in subsets of patients with common variable immunodeficiency. Clin. Exp. Immunol. *156*, 446–454.
14. Fevang, B., Yndestad, A., Sandberg, W.J., Holm, A.M., Müller, F., Aukrust, P., and Frøland, S.S. (2007). Low numbers of regulatory T cells in common variable immunodeficiency: association with chronic inflammation in vivo. Clin. Exp. Immunol. *147*, 521–525.
15. Schubert, D., Bode, C., Kenefeck, R., Hou, T.Z., Wing, J.B., Kennedy, A., Bulashevska, A., Petersen, B.S., Schäffer, A.A., Grüning, B.A., et al. (2014). Autosomal dominant immune dysregulation syndrome in humans with CTLA4 mutations. Nat. Med. *20*, 1410–1416.
16. Gathmann, B., Mahlaoui, N., Gérard, L., Oksenhendler, E., Warnatz, K., Schulze, I., Kindle, G., Kuijpers, T.W., van Beem, R.T., Guzman, D., et al.; CEREDIH; Dutch WID; European Society for Immunodeficiencies Registry Working Party (2014). Clinical picture and treatment of 2212 patients with common variable immunodeficiency. J. Allergy Clin. Immunol. *134*, 116–126.
17. Salzer, U., Unger, S., and Warnatz, K. (2012). Common variable immunodeficiency (CVID): exploring the multiple dimensions of a heterogeneous disease. Ann. N Y Acad. Sci. *1250*, 41–49.
18. Perkins, N.D. (2007). Integrating cell-signalling pathways with NF-kappaB and IKK function. Nat. Rev. Mol. Cell Biol. *8*, 49–62.
19. Courtois, G., and Gilmore, T.D. (2006). Mutations in the NF-kappaB signaling pathway: implications for human disease. Oncogene *25*, 6831–6843.
20. Orange, J.S., Levy, O., and Geha, R.S. (2005). Human disease resulting from gene mutations that interfere with appropriate nuclear factor-kappaB activation. Immunol. Rev. *203*, 21–37.
21. Hayden, M.S., and Ghosh, S. (2011). NF-κB in immunobiology. Cell Res. *21*, 223–244.
22. Bendall, H.H., Sikes, M.L., Ballard, D.W., and Oltz, E.M. (1999). An intact NF-kappa B signaling pathway is required for maintenance of mature B cell subsets. Mol. Immunol. *36*, 187–195.
23. Gugasyan, R., Grumont, R., Grossmann, M., Nakamura, Y., Pohl, T., Nesic, D., and Gerondakis, S. (2000). Rel/NF-kappaB transcription factors: key mediators of B-cell activation. Immunol. Rev. *176*, 134–140.
24. Pereira, S.G., and Oakley, F. (2008). Nuclear factor-kappaB1: regulation and function. Int. J. Biochem. Cell Biol. *40*, 1425–1430.
25. Gasparini, C., Celeghini, C., Monasta, L., and Zauli, G. (2014). NF-κB pathways in hematological malignancies. Cell. Mol. Life Sci. *71*, 2083–2102.
26. Karin, M. (2009). NF-kappaB as a critical link between inflammation and cancer. Cold Spring Harb. Perspect. Biol. *1*, a000141.
27. Yoshioka, T., Nishikomori, R., Hara, J., Okada, K., Hashii, Y., Okafuji, I., Nodomi, S., Kawai, T., Izawa, K., Ohnishi, H., et al. (2013). Autosomal dominant anhidrotic ectodermal dysplasia with immunodeficiency caused by a novel NFKBIA mutation, p.Ser36Tyr, presents with mild ectodermal dysplasia and non-infectious systemic inflammation. J. Clin. Immunol. *33*, 1165–1174.
28. Courtois, G., Smahi, A., Reichenbach, J., Döffinger, R., Cancrini, C., Bonnet, M., Puel, A., Chable-Bessia, C., Yamaoka, S., Feinberg, J., et al. (2003). A hypermorphic IkappaBalpha mutation is associated with autosomal dominant anhidrotic ectodermal dysplasia and T cell immunodeficiency. J. Clin. Invest. *112*, 1108–1115.
29. Burns, S.O., Plagnol, V., Gutierrez, B.M., Al Zahrani, D., Curtis, J., Gaspar, M., Hassan, A., Jones, A.M., Malone, M., Rampling, D., et al. (2014). Immunodeficiency and disseminated mycobacterial infection associated with homozygous nonsense mutation of IKKβ. J. Allergy Clin. Immunol. *134*, 215–218.
30. Mousallem, T., Yang, J., Urban, T.J., Wang, H., Adeli, M., Parrott, R.E., Roberts, J.L., Goldstein, D.B., Buckley, R.H., and Zhong, X.P. (2014). A nonsense mutation in IKBKB causes combined immunodeficiency. Blood *124*, 2046–2050.
31. Pannicke, U., Baumann, B., Fuchs, S., Henneke, P., Rensing-Ehl, A., Rizzi, M., Janda, A., Hese, K., Schlesier, M., Holzmann, K., et al. (2013). Deficiency of innate and acquired immunity caused by an IKBKB mutation. N. Engl. J. Med. *369*, 2504–2514.
32. Döffinger, R., Smahi, A., Bessia, C., Geissmann, F., Feinberg, J., Durandy, A., Bodemer, C., Kenwrick, S., Dupuis-Girod, S., Blanche, S., et al. (2001). X-linked anhidrotic ectodermal dysplasia with immunodeficiency is caused by impaired NF-kappaB signaling. Nat. Genet. *27*, 277–285.
33. Jain, A., Ma, C.A., Liu, S., Brown, M., Cohen, J., and Strober, W. (2001). Specific missense mutations in NEMO result in hyper-IgM syndrome with hypohydrotic ectodermal dysplasia. Nat. Immunol. *2*, 223–228.
34. Glocker, E.O., Hennigs, A., Nabavi, M., Schäffer, A.A., Woellner, C., Salzer, U., Pfeifer, D., Veelken, H., Warnatz, K., Tahami, F., et al. (2009). A homozygous CARD9 mutation in a family

with susceptibility to fungal infections. N. Engl. J. Med. *361*, 1727–1735.
35. Stepensky, P., Keller, B., Buchta, M., Kienzler, A.K., Elpeleg, O., Somech, R., Cohen, S., Shachar, I., Miosge, L.A., Schlesier, M., et al. (2013). Deficiency of caspase recruitment domain family, member 11 (CARD11), causes profound combined immunodeficiency in human subjects. J. Allergy Clin. Immunol. *131*, 477–85.e1.
36. Ogura, Y., Bonen, D.K., Inohara, N., Nicolae, D.L., Chen, F.F., Ramos, R., Britton, H., Moran, T., Karaliuskas, R., Duerr, R.H., et al. (2001). A frameshift mutation in NOD2 associated with susceptibility to Crohn's disease. Nature *411*, 603–606.
37. Hugot, J.P., Chamaillard, M., Zouali, H., Lesage, S., Cézard, J.P., Belaiche, J., Almer, S., Tysk, C., O'Morain, C.A., Gassull, M., et al. (2001). Association of NOD2 leucine-rich repeat variants with susceptibility to Crohn's disease. Nature *411*, 599–603.
38. Dowds, T.A., Masumoto, J., Zhu, L., Inohara, N., and Núñez, G. (2004). Cryopyrin-induced interleukin 1beta secretion in monocytic cells: enhanced activity of disease-associated mutants and requirement for ASC. J. Biol. Chem. *279*, 21924–21928.
39. Gerondakis, S., Grumont, R., Gugasyan, R., Wong, L., Isomura, I., Ho, W., and Banerjee, A. (2006). Unravelling the complexities of the NF-kappaB signalling pathway using mouse knockout and transgenic models. Oncogene *25*, 6781–6799.
40. Borm, M.E., van Bodegraven, A.A., Mulder, C.J., Kraal, G., and Bouma, G. (2005). A NFKB1 promoter polymorphism is involved in susceptibility to ulcerative colitis. Int. J. Immunogenet. *32*, 401–405.
41. Karban, A.S., Okazaki, T., Panhuysen, C.I., Gallegos, T., Potter, J.J., Bailey-Wilson, J.E., Silverberg, M.S., Duerr, R.H., Cho, J.H., Gregersen, P.K., et al. (2004). Functional annotation of a novel NFKB1 promoter polymorphism that increases risk for ulcerative colitis. Hum. Mol. Genet. *13*, 35–45.
42. Kaileh, M., and Sen, R. (2012). NF-κB function in B lymphocytes. Immunol. Rev. *246*, 254–271.
43. Gerondakis, S., and Siebenlist, U. (2010). Roles of the NF-kappaB pathway in lymphocyte development and function. Cold Spring Harb. Perspect. Biol. *2*, a000182.
44. Salzer, U., and Grimbacher, B. (2005). TACItly changing tunes: farewell to a yin and yang of BAFF receptor and TACI in humoral immunity? New genetic defects in common variable immunodeficiency. Curr. Opin. Allergy Clin. Immunol. *5*, 496–503.
45. von Bülow, G.U., Russell, H., Copeland, N.G., Gilbert, D.J., Jenkins, N.A., and Bram, R.J. (2000). Molecular cloning and functional characterization of murine transmembrane activator and CAML interactor (TACI) with chromosomal localization in human and mouse. Mamm. Genome *11*, 628–632.
46. Lougaris, V., Tabellini, G., Vitali, M., Baronio, M., Patrizi, O., Tampella, G., Biasini, A., Moratto, D., Parolini, S., and Plebani, A. (2015). Defective natural killer-cell cytotoxic activity in NFKB2-mutated CVID-like disease. J. Allergy Clin. Immunol. *135*, 1641–1643.e3. http://dx.doi.org/10.1016/j.jaci.2014.11.038.
47. Brue, T., Quentien, M.H., Khetchoumian, K., Bensa, M., Capo-Chichi, J.M., Delemer, B., Balsalobre, A., Nassif, C., Papadimitriou, D.T., Pagnier, A., et al. (2014). Mutations in NFKB2 and potential genetic heterogeneity in patients with DAVID syndrome, having variable endocrine and immune deficiencies. BMC Med. Genet. *15*, 139.
48. Lee, C.E., Fulcher, D.A., Whittle, B., Chand, R., Fewings, N., Field, M., Andrews, D., Goodnow, C.C., and Cook, M.C. (2014). Autosomal-dominant B-cell deficiency with alopecia due to a mutation in NFKB2 that results in nonprocessable p100. Blood *124*, 2964–2972.
49. Lindsley, A.W., Qian, Y., Valencia, C.A., Shah, K., Zhang, K., and Assa'ad, A. (2014). Combined immune deficiency in a patient with a novel NFKB2 mutation. J. Clin. Immunol. *34*, 910–915.
50. Liu, Y., Hanson, S., Gurugama, P., Jones, A., Clark, B., and Ibrahim, M.A. (2014). Novel NFKB2 mutation in early-onset CVID. J. Clin. Immunol. *34*, 686–690.
51. Chen, K., Coonrod, E.M., Kumánovics, A., Franks, Z.F., Durtschi, J.D., Margraf, R.L., Wu, W., Heikal, N.M., Augustine, N.H., Ridge, P.G., et al. (2013). Germline mutations in NFKB2 implicate the noncanonical NF-κB pathway in the pathogenesis of common variable immunodeficiency. Am. J. Hum. Genet. *93*, 812–824.
52. Finck, A., Van der Meer, J.W., Schäffer, A.A., Pfannstiel, J., Fieschi, C., Plebani, A., Webster, A.D., Hammarström, L., and Grimbacher, B. (2006). Linkage of autosomal-dominant common variable immunodeficiency to chromosome 4q. Eur. J. Hum. Genet. *14*, 867–875.
53. Andrews, N.C., and Faller, D.V. (1991). A rapid micropreparation technique for extraction of DNA-binding proteins from limiting numbers of mammalian cells. Nucleic Acids Res. *19*, 2499.
54. Li, H., and Durbin, R. (2009). Fast and accurate short read alignment with Burrows-Wheeler transform. Bioinformatics *25*, 1754–1760.
55. McKenna, A., Hanna, M., Banks, E., Sivachenko, A., Cibulskis, K., Kernytsky, A., Garimella, K., Altshuler, D., Gabriel, S., Daly, M., and DePristo, M.A. (2010). The Genome Analysis Toolkit: a MapReduce framework for analyzing next-generation DNA sequencing data. Genome Res. *20*, 1297–1303.
56. DePristo, M.A., Banks, E., Poplin, R., Garimella, K.V., Maguire, J.R., Hartl, C., Philippakis, A.A., del Angel, G., Rivas, M.A., Hanna, M., et al. (2011). A framework for variation discovery and genotyping using next-generation DNA sequencing data. Nat. Genet. *43*, 491–498.
57. Nijenhuis, T., Klasen, I., Weemaes, C.M., Preijers, F., de Vries, E., and van der Meer, J.W. (2001). Common variable immunodeficiency (CVID) in a family: an autosomal dominant mode of inheritance. Neth. J. Med. *59*, 134–139.
58. Moorthy, A.K., Savinova, O.V., Ho, J.Q., Wang, V.Y., Vu, D., and Ghosh, G. (2006). The 20S proteasome processes NF-kappaB1 p105 into p50 in a translation-independent manner. EMBO J. *25*, 1945–1956.
59. McDonald, D.R., Mooster, J.L., Reddy, M., Bawle, E., Secord, E., and Geha, R.S. (2007). Heterozygous N-terminal deletion of IkappaBalpha results in functional nuclear factor kappaB haploinsufficiency, ectodermal dysplasia, and immune deficiency. J. Allergy Clin. Immunol. *120*, 900–907.
60. Romberg, N., Virdee, M., Chamberlain, N., Oe, T., Schickel, J.N., Perkins, T., Cantaert, T., Rachid, R., Rosengren, S., Palazzo, R., et al. (2015). TNF receptor superfamily member 13b (TNFRSF13B) hemizygosity reveals transmembrane activator and CAML interactor haploinsufficiency at later stages of B-cell development. J. Allergy Clin. Immunol. http://dx.doi.org/10.1016/j.jaci.2015.05.012, S0091-6749(15)00716-2.
61. Chinen, J., Martinez-Gallo, M., Gu, W., Cols, M., Cerutti, A., Radigan, L., Zhang, L., Potocki, L., Withers, M., Lupski, J.R.,

and Cunningham-Rundles, C. (2011). Transmembrane activator and CAML interactor (TACI) haploinsufficiency results in B-cell dysfunction in patients with Smith-Magenis syndrome. J. Allergy Clin. Immunol. *127*, 1579–1586.

62. Kuehn, H.S., Ouyang, W., Lo, B., Deenick, E.K., Niemela, J.E., Avery, D.T., Schickel, J.N., Tran, D.Q., Stoddard, J., Zhang, Y., et al. (2014). Immune dysregulation in human subjects with heterozygous germline mutations in CTLA4. Science *345*, 1623–1627.
63. Boland, B.S., Widjaja, C.E., Banno, A., Zhang, B., Kim, S.H., Stoven, S., Peterson, M.R., Jones, M.C., Su, H.I., Crowe, S.E., et al. (2015). Immunodeficiency and autoimmune enterocolopathy linked to NFAT5 haploinsufficiency. J. Immunol. *194*, 2551–2560.
64. Capitani, N., Ariani, F., Amedei, A., Pezzicoli, A., Matucci, A., Vultaggio, A., Troilo, A., Renieri, A., Baldari, C.T., and D' Elios, M.M. (2012). Vav1 haploinsufficiency in a common variable immunodeficiency patient with defective T-cell function. Int. J. Immunopathol. Pharmacol. *25*, 811–817.
65. Hsu, A.P., Sampaio, E.P., Khan, J., Calvo, K.R., Lemieux, J.E., Patel, S.Y., Frucht, D.M., Vinh, D.C., Auth, R.D., Freeman, A.F., et al. (2011). Mutations in GATA2 are associated with the autosomal dominant and sporadic monocytopenia and mycobacterial infection (MonoMAC) syndrome. Blood *118*, 2653–2655.
66. Rieux-Laucat, F., and Casanova, J.L. (2014). Immunology. Autoimmunity by haploinsufficiency. Science *345*, 1560–1561.
67. Al-Herz, W., Bousfiha, A., Casanova, J.L., Chatila, T., Conley, M.E., Cunningham-Rundles, C., Etzioni, A., Franco, J.L., Gaspar, H.B., Holland, S.M., et al. (2014). Primary immunodeficiency diseases: an update on the classification from the international union of immunological societies expert committee for primary immunodeficiency. Front. Immunol. *5*, 162.
68. Sha, W.C., Liou, H.C., Tuomanen, E.I., and Baltimore, D. (1995). Targeted disruption of the p50 subunit of NF-kappa B leads to multifocal defects in immune responses. Cell *80*, 321–330.
69. Bernal, G.M., Wahlstrom, J.S., Crawley, C.D., Cahill, K.E., Pytel, P., Liang, H., Kang, S., Weichselbaum, R.R., and Yamini, B. (2014). Loss of Nfkb1 leads to early onset aging. Aging (Albany, N.Y.) *6*, 931–943.